Macroscopic permeability of doubly porous solids with spheroidal macropores: close form approximate solutions of the longitudinal permeability

Vincent Monchiet

Macroscopic permeability of doubly porous solids with spheroidal macropores: close form approximate solutions of the longitudinal permeability

By Vincent Monchiet

Univ Gustave Eiffel, Univ Paris Est Creteil, CNRS, MSME UMR 8208, F-77454 Marne-la-Vallée, France

The presence of macropores and fractures significantly affects the effective transport properties of porous solids such as concrete or rocks. The dimensions of the fractures are generally large behind that of the initial porosity, so that the problem contains two porosities. The influence of the macroporosity is studied in the homogenization framework by solving at the intermediate scale, that of the macropores, a coupled Darcy/Stokes problem with the Beavers-Joseph-Saffman (BJS) interface condition. We derive analytic expressions of the macroscopic permeability in the case of an isotropic permeable matrix containing spheroidal shaped macropores. To this aim, we consider a Representative Volume Element (RVE) on which uniform boundary conditions are considered for the velocity and pressure fields. The local problem is written as minimum principles; kinematic and static approaches are developed in order to derive rigorous bounds for the macroscopic permeability. Close form expressions of the longitudinal permeability (along the revolution axe of the spheroid) are determined by considering a simplified RVE constituted of two confocal spheroids. They depend on the volume fraction and the eccentricity of the spheroidal macropores, the scale factor between the two porosities and the slip coefficient of the BJS model. Illustrations show the influence of these parameters.

Keywords: Biporous Solids, Spheroids, Permeability, Darcy, Stokes

1. Introduction

The determination of the effective permeability of biporous solids is of key importance for many practical problems. For instance, concrete and rocks are naturally biporous solids. Note that biporous polymers are used for various applications such as bio-implants (18; 19). The concept of the double porosity was introduced by Barrenblatt et al. (8) to study the transport properties when the solid is constituted of two populations of pores. To avoid any confusion, the smaller pores are called micropores. Conversely, the larger pores are called macropores, fractures or vugs. The solid is constituted of : (i) a homogeneous permeable matrix containing only the micropores and (ii) the macropores which are embedded in the permeable medium.

The development of homogenization techniques applied to biporous materials has been investigated by Auriault and Boutin (4; 5; 6), Royer et al. (31), Boutin et al.

(11), Olny & Boutin (26) considering the method based on a double asymptotic expansion series. When the fractures are sufficiently large relative to the micropores, a double upscaling approach can be applied and it has been found that the macroscopic permeability involves the resolution of a coupled Darcy/Stokes problem at the intermediate scale. The Darcy equation is used to describe the fluid flow in the permeable porous solid containing the micropores and the Stokes equations is related to the fluid flow in the fractures. Note that the asymptotic series expansion method do not deliver the interface conditions between the Darcy and the Stokes region.

Two strategies have been used to account for the boundary layer. The first consists use the Beavers-Joseph-Saffman (BJS) interfacial model (9; 32), the second one consists to replace the Darcy law in the permeable solid by the Brinkman equation (12; 13). The Brinkman model can simply be regarded as a transmission model, bridging the limits of open to very porous media. Specifically, by considering the fluid as a porous medium with very high permeability, the fluid/porous composite region can be treated with only the Brinkman equation, which helps circumventing the use of suitable conditions for the interface. Note that the Brinkman law introduces an effective viscosity. The determination of this parameter has been addressed in the framework of the asymptotic homogenization approach by Auriault et al. (7).

Many studies have been devoted to the resolution of the coupled Darcy/Stokes equations with various practical applications such as: fractured reservoir (27), flow in porous media with cracks (10), industrial filtration systems (17), etc.

More specifically, numerical studies have been widely used to investigate the fluid flow in porous solids with vugs (35; 36; 2; 22; 23) considering the coupled Darcy/Stokes equations with the BJS interfacial model and finite element or finite volume method for its numerical resolution.

An analytic expression of the macroscopic permeability has been first provided by Markov et al. (20) introducing the concept of equivalent permeability for the macropores. This equivalent permeability is determined by solving the coupled Darcy/Stokes equations with the BJS interface model for an isolated macropore fulfilled by a viscous fluid embedded in an infinite porous matrix. Next, by making use of the analogy between the Darcy equation and that of the thermal conductivity, the effective permeability is estimated by the formula of Maxwell (21). More recently, in Monchiet et al. (24), the solution of the coupled Darcy/Stokes equations with the BJS interface model has been solved for coaxial cylinders and spheres subjected to a uniform velocity or pressure gradient at its boundary. The inner cylinder and sphere represent the macropore embedded in a porous matrix. Note that the exact analytical solution for fluid flow in porous media including a single circular or slightly deformed circular-shaped vug was also obtained (28; 29). Note also that another analytic solutions has been derived for a composite cylinder (34), *i.e.* two concentric cylinders in which the flow obeys to the Brinkman equation but with different coefficients in the core and in the coating. More recently, the results of Markov et al. (20) have been latter to the case of a spheroidal cavity (30) by expanding the solution in series of functions of the spheroidal coordinates.

In the present paper, we propose to extend the work of Monchiet et al. (24) to the case of confocal spheroids. In the case of spheroidal shape, no exact solution has been found and to circumvent this difficulty we approximate the solution by considering two minimum principles. By choosing adequately the trial fields, the

macroscopic longitudinal permeability is determined from a kinematic and a static minimum principle, leading to a rigorous lower and upper bound respectively for the effective permeability of the biporous solid with spheroidal vugs.

2. Homogenization of doubly porous solid

(*a*) *Local equations and interface conditions*

Consider a Representative Volume Element (RVE) of a doubly porous solid. It is constituted of two phases: (i) a permeable matrix in which the fluid flow obeys to the Darcy law, (ii) macropores fulfilled by the same viscous fluid in which the fluid flow obeys to the Stokes equations. The dynamic viscosity of the fluid is denoted by μ. We denote by Ω_d the domain occupied by the porous solid (with micropores) and by Ω_s the domain of the macropores (the indices "s" and "d" make reference to "Stokes" and "Darcy"). The Darcy region is assumed to be isotropic and we denote by k its permeability that is assumed to be known (obtained from experiments or numerical simulations). We also define by $h = 1/k$ the hydraulic resistivity. The macropores are assumed to be non interconnected. Moreover, we also assume for simplicity that the macropores do not cross the boundary of the RVE. Denoting by d the characteristic length of the channels of the initial interconnected microporous solid (the micropores), we assume that d is sufficiently small compared to the characteristic length of the macropores, L, such that the scale separation condition between the two porosities is satisfied, $d << L$. Under this assumption, the macropores are then embedded in a homogenous permeable porous solid having the homogeneous permeability k.

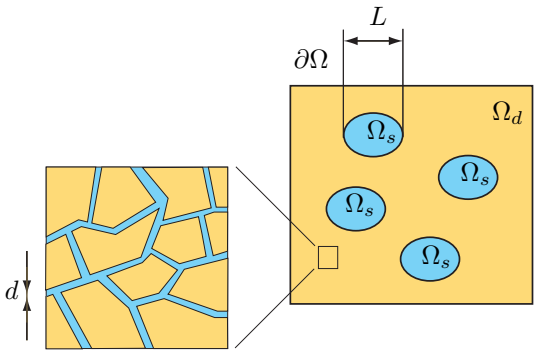

Figure 1. Schematic representation of the RVE

In the macropores, the fluid flow is described by the Stokes equations:

$$\mu\Delta\boldsymbol{v} - \nabla p = 0; \quad \operatorname{div}\boldsymbol{v} = 0 \quad \forall \boldsymbol{x} \in \Omega_s \tag{2.1}$$

Within the permeable solid, the fluid flow obeys to the Darcy law with the incompressibility condition:

$$\boldsymbol{v} = -\frac{k}{\mu}\nabla p; \quad \operatorname{div}\boldsymbol{v} = 0 \quad \forall \boldsymbol{x} \in \Omega_d \tag{2.2}$$

At the interface between the fluid and the solid, we use the interface model of Beavers and Joseph (9), Saffman (32) (called BJS model for simplicity). The interfaces conditions are:

- the continuity of the mass flux:

$$\boldsymbol{v}^d.\boldsymbol{\nu} = \boldsymbol{v}^s.\boldsymbol{\nu} \quad \forall \boldsymbol{x} \in \Gamma \tag{2.3}$$

- the discontinuity for the tangential velocity:

$$\boldsymbol{\nu}.\boldsymbol{\sigma}^s.\boldsymbol{\tau} = 2\mu\boldsymbol{\nu}.\boldsymbol{D}(\boldsymbol{v}^s).\boldsymbol{\tau} = -\lambda\boldsymbol{v}^s.\boldsymbol{\tau} \quad \forall \boldsymbol{x} \in \Gamma \tag{2.4}$$

- the continuity for the normal traction:

$$\boldsymbol{\nu}.\boldsymbol{\sigma}^s.\boldsymbol{\nu} = 2\mu\boldsymbol{\nu}.\boldsymbol{D}(\boldsymbol{v}^s).\boldsymbol{\nu} - p^s = -p^d \quad \forall \boldsymbol{x} \in \Gamma \tag{2.5}$$

in which p^s, $\boldsymbol{v}^s$ and p^d, $\boldsymbol{v}^d$ represent the pressure and velocity fields taken at each side of the interface Γ, exponent d makes reference to the Darcy region and s to the Stokes one. In equation (2.4), λ is a coefficient of the BJS model, $\boldsymbol{D}(\boldsymbol{v}^s)$ represents the strain rate tensor computed in the Stokes region, $\boldsymbol{\sigma}^s$ is the stress tensor defined by:

$$\boldsymbol{\sigma}^s = 2\mu\boldsymbol{D}(\boldsymbol{v}^s) - p^s\boldsymbol{I} \tag{2.6}$$

where $\boldsymbol{I}$ is the identity tensor. Also, $\boldsymbol{\nu}$ and $\boldsymbol{\tau}$ represent the normal and the tangential unit vectors acting on Γ.
Based on their experimental observations, Beavers & Joseph 1967 proposed the following expressions for the coefficient λ:

$$\lambda = \frac{\mu}{\sqrt{k}}\delta \tag{2.7}$$

in which δ is a dimensionless coefficient called "slip coefficient" and is characteristic of the geometry of the porous solid. This coefficient has been determined experimentally by Beavers and Joseph (9) for Nickel foametal and found 0.78, 1.45 and 4.0 for porous microstructures having average pore size of 0.016, 0.034 and 0.045 inches respectively. For Aloxite they found a value of 0.1 for the both average pore size of 0.013 and 0.027 inches. Numerical studies have been also provided by Sahraoui and Kaviany (33) for 2d periodic structure made of cylindrical particles and found a value of the slip coefficient closed to 2. Note that the existence and uniqueness of the solution of Darcy/Stokes coupled problem with the BJS interface condition has been studied for instance by Arbogast and Lehr (1).
Note also that the velocity field is divergence free in the porous solid and in the macropores. The pressure is then an harmonic function everywhere in the RVE:

$$\Delta p = 0 \quad \forall \underline{x} \in \Omega_d \cup \Omega_s \tag{2.8}$$

(*b*) *Boundary conditions and macroscopic permeability*

(i) *Uniform pressure gradient condition on the boundary*

In order to determine the macroscopic permeability of the porous material, let Ω be subjected to the following prescribed pressure on its external surface $\partial\Omega$:

$$p = \boldsymbol{J}.\boldsymbol{x}, \quad \forall \boldsymbol{x} \in \partial\Omega \tag{2.9}$$

where $\boldsymbol{J}$ represents the macroscopic pressure gradient. Due to the linearity of the coupled Darcy/Stokes equations, the local velocity linearly depends on the applied macroscopic pressure gradient $\boldsymbol{J}$. Let us introduce the localization tensor $\boldsymbol{A}(\boldsymbol{x})$ such that:

$$\boldsymbol{v}(\boldsymbol{x}) = \boldsymbol{A}(\boldsymbol{x}).\boldsymbol{J} \tag{2.10}$$

The macroscopic velocity is obtained by the averaging rule:

$$\boldsymbol{V} =< \boldsymbol{v}(\boldsymbol{x}) >_\Omega = -\frac{1}{\mu}\boldsymbol{K}^{hom}.\boldsymbol{J} \tag{2.11}$$

where $<>_\Omega$ denotes the volume average over the volume Ω. The macroscopic permeability is given by:

$$\boldsymbol{K}^{hom} = -\mu < \boldsymbol{A}(\boldsymbol{x}) >_\Omega \tag{2.12}$$

(ii) *Uniform velocity condition on the boundary*

The following boundary condition is considered on the external surface of the RVE:

$$\boldsymbol{v}.\boldsymbol{n} = \boldsymbol{V}.\boldsymbol{n}, \quad \forall \boldsymbol{x} \in \partial\Omega \tag{2.13}$$

in which $\boldsymbol{n}$ is the normal unit vector taken on the boundary $\partial\Omega$.
Due to the linearity of the equations, the local pressure field can be read in the form:

$$p(\boldsymbol{x}) = \boldsymbol{B}(\boldsymbol{x}).\boldsymbol{V} \tag{2.14}$$

The pressure field being discontinuous across the interface Γ, the following definition is used for the average gradient of pressure:

$$\boldsymbol{J} =< \nabla p(\boldsymbol{x}) >_\Omega + \frac{1}{|\Omega|}\int_\Gamma [p(\boldsymbol{x})]\boldsymbol{\nu} dx \tag{2.15}$$

where $[p(\boldsymbol{x})] = p^d(\boldsymbol{x}) - p^s(\boldsymbol{x})$ represents the jump of $p(\boldsymbol{x})$ across Γ. Note that Eq. (2.15) can be also read:

$$\boldsymbol{J} = \frac{1}{|\Omega|}\int_{\partial\Omega} p(\boldsymbol{x})\boldsymbol{n} dx \tag{2.16}$$

Introducing Eq. (2.14) in Eq. (2.15), it leads to:

$$\boldsymbol{J} = -\mu\boldsymbol{H}^{hom}.\boldsymbol{V} \tag{2.17}$$

where $\boldsymbol{H}^{hom}$ is the macroscopic hydraulic resistivity, the inverse of $\boldsymbol{K}^{hom}$ that is given by:

$$\boldsymbol{H}^{hom} = -\frac{1}{\mu}\left\{< \nabla\boldsymbol{B}(\boldsymbol{x}) >_\Omega + \frac{1}{|\Omega|}\int_\Gamma \boldsymbol{\nu} \overset{s}{\otimes} [\boldsymbol{B}(\boldsymbol{x})] dx\right\} \tag{2.18}$$

3. Minimum principles

(*a*) *First minimum principle : kinematic approach*

In this section, we derive the variational procedure in order to deliver a lower bound for the macroscopic permeability (then an upper bound for the hydraulic

resistivity) of the biporous solid. This variational principle is called kinematic approach since it uses the velocity as trial fields. Let us first consider the problem for which the solid is subjected to a macroscopic velocity $\boldsymbol{V}$ by applying the uniform boundary condition described by Eq. (2.13). We denote by $\mathcal{V}$ the set of admissible velocity fields which are:

- (i) continuous and derivable in Ω_s and Ω_d,
- (ii) which satisfy to the boundary condition (2.13),
- (iii) are divergence free,
- (iv) which comply with continuity of the normal velocity across the interface Γ (see Eq. (2.3)).

Let us also introduce the functional $W(\boldsymbol{v})$ defined by:

$$W(\boldsymbol{v}) = \frac{1}{|\Omega|}\int_{\Omega_d}\frac{\mu h}{2}\boldsymbol{v}^d.\boldsymbol{v}^d dV + \frac{1}{|\Omega|}\int_{\Gamma}\frac{\lambda}{2}(\boldsymbol{v}^s.\boldsymbol{\tau})^2 dS + \frac{1}{|\Omega|}\int_{\Omega_s}\mu\boldsymbol{D}(\boldsymbol{v}^s):\boldsymbol{D}(\boldsymbol{v}^s)dV \tag{3.1}$$

where it is recalled that $\boldsymbol{v}^s$ and $\boldsymbol{v}^d$ represent the velocity in the Stokes and in the Darcy region respectively. Denoting by $\boldsymbol{v}$ the solution of the Darcy-Stokes problem with the boundary condition (2.13), we have:

$$W(\boldsymbol{v}) = \frac{\mu}{2}\boldsymbol{V}.\boldsymbol{H}^{hom}.\boldsymbol{V} = \min_{\widetilde{\boldsymbol{v}}\in\mathcal{V}} W(\widetilde{\boldsymbol{v}}) \tag{3.2}$$

It is then possible to derive an upper bound for the macroscopic hydraulic resistivity, then an lower bound for the macroscopic permeability $\boldsymbol{K}^{hom}$ considering an admissible velocity field $\widetilde{\boldsymbol{v}}$.

Proof:
The first variation of the potential $W(\boldsymbol{v})$ is:

$$\begin{aligned}\delta W(\boldsymbol{v}) = \frac{1}{|\Omega|}\int_{\Omega_d}\mu h\boldsymbol{v}^d.\delta\boldsymbol{v}dV + \frac{1}{|\Omega|}\int_{\Gamma}\lambda(\boldsymbol{v}^s.\boldsymbol{\tau})(\delta\boldsymbol{v}^s.\boldsymbol{\tau})dS \\ + \frac{1}{|\Omega|}\int_{\Omega_s}2\mu\boldsymbol{D}(\boldsymbol{v}^s):\boldsymbol{D}(\delta\boldsymbol{v}^s)dV\end{aligned} \tag{3.3}$$

in which $\delta\boldsymbol{v} = \boldsymbol{v} - \widetilde{\boldsymbol{v}}$ satisfies to $\delta\boldsymbol{v} = 0$ on the boundary $\partial\Omega$.
We aim to show that $\delta W(\boldsymbol{v}) = 0$. In Ω_d, we have $\boldsymbol{v}^d = -k/\mu\nabla p^d$, it follows that the first integral in Eq. (3.3) can be also read (considering that $h = 1/k$):

$$\int_{\Omega_d}\mu h\boldsymbol{v}^d.\delta\boldsymbol{v}^d dV = -\int_{\partial\Omega}p^d(\delta\boldsymbol{v}^d.\boldsymbol{n})dS + \int_{\Gamma}p^d(\delta\boldsymbol{v}^d.\boldsymbol{\nu})dS \tag{3.4}$$

Owing to the property $\delta\boldsymbol{v} = 0$ on the boundary $\partial\Omega$, we deduce that:

$$\int_{\Omega_d}\mu h\boldsymbol{v}^d.\delta\boldsymbol{v}^d dV = \int_{\Gamma}p^d(\delta\boldsymbol{v}^d.\boldsymbol{\nu})dS \tag{3.5}$$

The last integral in Eq. (3.3) can be read:

$$\int_{\Omega_s}2\mu\boldsymbol{D}(\boldsymbol{v}^s):\boldsymbol{D}(\delta\boldsymbol{v}^s)dV = \int_{\Gamma}2\mu\delta\boldsymbol{v}^s.\boldsymbol{D}(\boldsymbol{v}^s).\boldsymbol{\nu}dS - \int_{\Gamma}2\mu\,\mathrm{div}(\boldsymbol{D}(\boldsymbol{v}^s)).\delta\boldsymbol{v}^s dV \tag{3.6}$$

Moreover, $\boldsymbol{v}^s$ being divergence free, we have $\mathrm{div}(\boldsymbol{D}(\boldsymbol{v}^s)) = \frac{1}{2}\Delta\boldsymbol{v}^s$. Since $\boldsymbol{v}^s$ satisfies to the Stokes equations, we have also $\mu\Delta\boldsymbol{v}^s = \nabla p^s$. As a consequence, the above integral can be also put into the form:

$$\int_{\Omega_s} 2\mu\boldsymbol{D}(\boldsymbol{v}^s) : \boldsymbol{D}(\delta\boldsymbol{v}^s)dV = \int_\Gamma 2\mu\delta\boldsymbol{v}^s.\boldsymbol{D}(\boldsymbol{v}^s).\boldsymbol{\nu}dS - \int_{\Omega_s} \nabla p^s.\delta\boldsymbol{v}^s dV \tag{3.7}$$

$\delta\boldsymbol{v}^s$ being divergence free, we have $\nabla p^s.\delta\boldsymbol{v}^s = \mathrm{div}(p^s\delta\boldsymbol{v}^s)$. This implies:

$$\int_{\Omega_s} 2\mu\boldsymbol{D}(\boldsymbol{v}^s) : \boldsymbol{D}(\delta\boldsymbol{v}^s)dV = \int_\Gamma 2\mu\delta\boldsymbol{v}^s.\boldsymbol{D}(\boldsymbol{v}^s).\boldsymbol{\nu}dS - \int_\Gamma p^s\delta\boldsymbol{v}^s.\boldsymbol{\nu}dS \tag{3.8}$$

Considering Eqs. (3.5) and (3.8) in Eq. (3.3), we obtain:

$$\begin{aligned}\delta W(\boldsymbol{v}) = &\frac{1}{|\Omega|}\int_\Gamma p^d(\delta\boldsymbol{v}^d.\boldsymbol{\nu})dS + \frac{1}{|\Omega|}\int_\Gamma \lambda(\boldsymbol{v}^s.\boldsymbol{\tau})(\delta\boldsymbol{v}^s.\boldsymbol{\tau})dS \\ &+\frac{1}{|\Omega|}\int_\Gamma 2\mu\delta\boldsymbol{v}^s.\boldsymbol{D}(\boldsymbol{v}^s).\boldsymbol{\nu}dS - \frac{1}{|\Omega|}\int_\Gamma p^s\delta\boldsymbol{v}^s.\boldsymbol{\nu}ds\end{aligned} \tag{3.9}$$

On Γ, the velocity $\delta\boldsymbol{v}^s$ can be decomposed into its normal and tangential components:

$$\delta\boldsymbol{v}^s = (\delta\boldsymbol{v}^s.\boldsymbol{\tau})\boldsymbol{\tau} + (\delta\boldsymbol{v}^s.\boldsymbol{\nu})\boldsymbol{\nu} \tag{3.10}$$

The normal component of $\delta\boldsymbol{v}$ is continuous across Γ, $\delta\boldsymbol{v}^d.\boldsymbol{n} = \delta\boldsymbol{v}^s.\boldsymbol{n}$, this leading for Eq. (3.9) to:

$$\begin{aligned}\delta W(\boldsymbol{v}) = &\frac{1}{|\Omega|}\int_\Gamma \left[2\mu\boldsymbol{\nu}.\boldsymbol{D}(\boldsymbol{v}^s).\boldsymbol{\nu} + p^d - p^s\right](\delta\boldsymbol{v}^d.\boldsymbol{\nu})dS \\ &+\frac{1}{|\Omega|}\int_\Gamma \left[2\mu\boldsymbol{\tau}.\boldsymbol{D}(\boldsymbol{v}^s).\boldsymbol{\nu} + \lambda\boldsymbol{v}^s.\boldsymbol{\tau}\right](\delta\boldsymbol{v}^s.\boldsymbol{\tau})dS\end{aligned} \tag{3.11}$$

The two integrals in the above equation are null considering Eq. (2.4) and Eq. (2.5). The solution of the Darcy-Stokes problem $\boldsymbol{v}$ is a stationary point of W. Moreover, if h, μ and λ are strictly positive, then W is convex. Thereby the solution of the coupled Darcy/Stokes problem $\boldsymbol{v}$ is a global minimum of W.
The second part of the proof consists to prove that:

$$W(\boldsymbol{v}) = \frac{\mu}{2}\boldsymbol{V}.\boldsymbol{H}^{hom}.\boldsymbol{V} \tag{3.12}$$

In Ω_d, if we replace $\boldsymbol{v}^d$ by $-k/\mu\nabla p^d$, it gives:

$$\int_{\Omega_d} \frac{\mu h}{2}\boldsymbol{v}^d.\boldsymbol{v}^d dV = -\int_{\partial\Omega} \frac{1}{2}p^d(\boldsymbol{v}^d.\boldsymbol{n})dS + \int_\Gamma \frac{1}{2}p^d(\boldsymbol{v}^d.\boldsymbol{\nu})dS \tag{3.13}$$

Because $\boldsymbol{v}^s$ satisfies to the Stokes equations, we have:

$$\int_{\Omega_s} \mu\boldsymbol{D}(\boldsymbol{v}^s) : \boldsymbol{D}(\boldsymbol{v}^s)dV = \mu\int_\Gamma \boldsymbol{v}^s.\boldsymbol{D}(\boldsymbol{v}^s).\boldsymbol{\nu}dS - \frac{1}{2}\int_\Gamma p^s(\boldsymbol{v}^s.\boldsymbol{\nu})dV \tag{3.14}$$

Considering Eqs. (3.13) and (3.14) in Eq. (3.1) with the interface conditions (2.3), (2.4) and (2.5) we obtain:

$$W(\boldsymbol{v}) = -\frac{1}{2}\int_{\partial\Omega} p^d(\boldsymbol{v}^d.\boldsymbol{n})dS \tag{3.15}$$

Owing to the boundary condition $\boldsymbol{v}.\boldsymbol{n} = \boldsymbol{V}.\boldsymbol{n}$ we deduce that:

$$W(\boldsymbol{v}) = -\frac{1}{2}\boldsymbol{V}.\int_{\partial\Omega} p^d\boldsymbol{n}dS \tag{3.16}$$

Considering Eq. (2.16) we deduce that:

$$W(\boldsymbol{v}) = -\frac{1}{2}\boldsymbol{V}.\boldsymbol{J} = \frac{\mu}{2}\boldsymbol{V}.\boldsymbol{H}^{hom}.\boldsymbol{V} \tag{3.17}$$

(b) Complementary minimum principle : static approach

A complementary variational principle can be derived by considering the admissible pair $(\widehat{p}^d, \widetilde{\boldsymbol{\sigma}}^s) \in \mathcal{S}$ such that:

- $\widehat{p}^d$ and $\widetilde{\boldsymbol{\sigma}}^s$ are continuous and derivable in Ω_d and Ω_s,
- $\widetilde{\boldsymbol{\sigma}}^s$ is divergence free in Ω_s,
- $\widehat{p}^d$ and $\widetilde{\boldsymbol{\sigma}}^s$ comply with the continuity of the traction: $\boldsymbol{\nu}.\widetilde{\boldsymbol{\sigma}}^s.\boldsymbol{\nu} = -\widetilde{p}^d$ on Γ,
- $\widehat{p}^d$ satisfies to the uniform pressure gradient boundary condition $\widetilde{p}^d = \boldsymbol{J}.\boldsymbol{x}$ on $\partial\Omega$.

This complementary variational principle leads to an upper bound for the macroscopic permeability of the biporous solid, then a lower bound for the resistivity. This variational principle is also called static approach since it uses the pressure in the Darcy region and the stress in the Stokes region as trial fields.
The complementary variational principle reads:

$$W^*(p^d, \boldsymbol{\sigma}^s) = \frac{1}{2\mu}\boldsymbol{J}.\boldsymbol{K}^{hom}.\boldsymbol{J} = \min_{(\widehat{p}^d,\widetilde{\boldsymbol{\sigma}}^s)\in\mathcal{S}} W^*(\widetilde{p}^d, \widetilde{\boldsymbol{\sigma}}^s) \tag{3.18}$$

where $W^*(p^d, \boldsymbol{\sigma}^s)$ is defined by:

$$\begin{aligned} W^*(p^d, \boldsymbol{\sigma}^s) = \frac{1}{|\Omega|}\int_{\Omega_d}\frac{k}{2\mu}\nabla p^d.\nabla p^d dV + \frac{1}{|\Omega|}\int_\Gamma \frac{1}{2\lambda}(\boldsymbol{\nu}.\boldsymbol{\sigma}^s.\boldsymbol{\tau})^2 dS \\ + \frac{1}{|\Omega|}\int_{\Omega_s}\frac{1}{4\mu}\overline{\boldsymbol{\sigma}}^s : \overline{\boldsymbol{\sigma}}^s dV \end{aligned} \tag{3.19}$$

where $\overline{\boldsymbol{\sigma}}^s$ represents the deviatoric part of $\boldsymbol{\sigma}^s$.

Proof:
Consider the first variation of W^*:

$$\begin{aligned} \delta W^*(p^d, \boldsymbol{\sigma}^s) = \frac{1}{|\Omega|}\int_{\Omega_d}\frac{k}{\mu}\nabla p^d.\nabla \delta p^d dV + \frac{1}{|\Omega|}\int_\Gamma \frac{1}{\lambda}(\boldsymbol{\nu}.\boldsymbol{\sigma}^s.\boldsymbol{\tau})(\boldsymbol{\nu}.\delta\boldsymbol{\sigma}^s.\boldsymbol{\tau}) dS \\ + \frac{1}{|\Omega|}\int_{\Omega_s}\frac{1}{2\mu}\overline{\boldsymbol{\sigma}}^s : \delta\overline{\boldsymbol{\sigma}}^s dV \end{aligned} \tag{3.20}$$

in which $\delta p^d = p^d - \widetilde{p}^d$ and $\delta\boldsymbol{\sigma}^s = \boldsymbol{\sigma}^s - \widetilde{\boldsymbol{\sigma}}^s$. Note that δp^d satisfies to $\delta p^d = 0$ on the boundary $\partial\Omega$. Additionally, the pressure p^d is Laplacian free, $\Delta p^d = 0$, consequently we have:

$$\int_{\Omega_d} \frac{k}{\mu} \nabla p^d . \nabla \delta p^d dV = -\int_\Gamma \frac{k}{\mu} (\nabla p^d . \boldsymbol{\nu}) \delta p^d dS \tag{3.21}$$

In the last integral in (3.20), we can replace $\overline{\boldsymbol{\sigma}}^s$ by $2\mu \boldsymbol{D}(\boldsymbol{v}^s)$. Because $\boldsymbol{D}(\boldsymbol{v}^s)$ is deviatoric, in the expression $\boldsymbol{D}(\boldsymbol{v}^s) : \delta\overline{\boldsymbol{\sigma}}^s$ the term $\delta\boldsymbol{\sigma}^s$ can be substituted to $\delta\overline{\boldsymbol{\sigma}}^s$. As a consequence, we can read:

$$\frac{1}{2\mu} \overline{\boldsymbol{\sigma}}^s : \delta\overline{\boldsymbol{\sigma}}^s = \boldsymbol{D}(\boldsymbol{v}^s) : \delta\boldsymbol{\sigma}^s \tag{3.22}$$

Since $\delta\boldsymbol{\sigma}^s$ is divergence free, we have:

$$\int_{\Omega_s} \frac{1}{2\mu} \overline{\boldsymbol{\sigma}}^s : \delta\overline{\boldsymbol{\sigma}}^s dV = \int_\Gamma \boldsymbol{v}^s . \delta\boldsymbol{\sigma}^s . \boldsymbol{\nu} dS \tag{3.23}$$

Owing to Eq. (3.21) and Eq. (3.23) in Eq. (3.20), we obtain:

$$\begin{aligned} \delta W^*(p^d, \boldsymbol{\sigma}^s) = \frac{1}{|\Omega|} \int_\Gamma \frac{k}{\mu} (\nabla p^d . \boldsymbol{\nu}) \delta p^d dS + \frac{1}{|\Omega|} \int_\Gamma \frac{1}{\lambda} (\boldsymbol{\nu} . \boldsymbol{\sigma}^s . \boldsymbol{\tau})(\boldsymbol{\nu} . \delta\boldsymbol{\sigma}^s . \boldsymbol{\tau}) dS \\ + \frac{1}{|\Omega|} \int_\Gamma \boldsymbol{v}^s . \delta\boldsymbol{\sigma}^s . \boldsymbol{\nu} dS \end{aligned} \tag{3.24}$$

The velocity is decomposed into its tangential and normal components:

$$\boldsymbol{v}^s = (\boldsymbol{v}^s . \boldsymbol{\tau})\boldsymbol{\tau} + (\boldsymbol{v}^s . \boldsymbol{\nu})\boldsymbol{\nu} \tag{3.25}$$

Eq. (3.24) then becomes:

$$\begin{aligned} \delta W^*(p^d, \boldsymbol{\sigma}^s) = -\frac{1}{|\Omega|} \int_\Gamma \frac{k}{\mu} (\nabla p^d . \boldsymbol{\nu}) \delta p^d dS + \frac{1}{|\Omega|} \int_\Gamma \frac{1}{\lambda} (\boldsymbol{\nu} . \boldsymbol{\sigma}^s . \boldsymbol{\tau})(\boldsymbol{\nu} . \delta\boldsymbol{\sigma}^s . \boldsymbol{\tau}) dS \\ + \frac{1}{|\Omega|} \int_\Gamma (\boldsymbol{v}^s . \boldsymbol{\nu})(\boldsymbol{\nu} . \delta\boldsymbol{\sigma}^s . \boldsymbol{\nu}) dS + \frac{1}{|\Omega|} \int_\Gamma (\boldsymbol{v}^s . \boldsymbol{\tau})(\boldsymbol{\tau} . \delta\boldsymbol{\sigma}^s . \boldsymbol{\nu}) dS \end{aligned} \tag{3.26}$$

In the first integral in Eq. (3.26), $k/\mu(\nabla p^d . \boldsymbol{\nu}) = -\boldsymbol{v}^d . \boldsymbol{\nu}$. The normal component of the velocity being continuous across Γ, we have $\boldsymbol{v}^s . \boldsymbol{\nu} = \boldsymbol{v}^d . \boldsymbol{\nu}$. Then Eq. (3.26) becomes:

$$\begin{aligned} \delta W^*(p^d, \boldsymbol{\sigma}^s) = \frac{1}{|\Omega|} \int_\Gamma (\boldsymbol{v}^s . \boldsymbol{\nu}) \left[\boldsymbol{\nu} . \delta\boldsymbol{\sigma}^s . \boldsymbol{\nu} + \delta p^d \right] dS \\ + \frac{1}{|\Omega|} \int_\Gamma \left[\frac{1}{\lambda} \boldsymbol{\nu} . \boldsymbol{\sigma}^s . \boldsymbol{\tau} + \boldsymbol{v}^s . \boldsymbol{\tau} \right] (\boldsymbol{\nu} . \delta\boldsymbol{\sigma}^s . \boldsymbol{\tau}) dS \end{aligned} \tag{3.27}$$

The first integral is null because δp^d and $\delta\boldsymbol{\sigma}^s$ satisfy to the continuity of the traction on Γ. The second integral is also null because $\boldsymbol{\sigma}^s$ and $\boldsymbol{v}^s$ satisfy to the BJS condition (see Eq. (2.4)). It follows that $\delta W^*(p^d, \boldsymbol{\sigma}^s) = 0$. Due to the convexity of W^*, the solution of the coupled Darcy/Stokes problem is a global minimum of W^*.
The second part of the demonstration consists to prove that:

$$W^*(p^d, \boldsymbol{\sigma}^s) = \frac{1}{2\mu} \boldsymbol{J} . \boldsymbol{K}^{hom} . \boldsymbol{J} \tag{3.28}$$

To this end, we replace, in the first integral in (3.19), $k/\mu\nabla p^d$ by $-\boldsymbol{v}^d$. It follows that:

$$\int_{\Omega_d} \frac{k}{2\mu}\nabla p^d.\nabla p^d dV = -\int_{\partial\Omega} \frac{1}{2}p^d(\boldsymbol{v}^d.\boldsymbol{n})dS + \int_{\Gamma} \frac{1}{2}p^d(\boldsymbol{v}^d.\boldsymbol{\nu})dS \tag{3.29}$$

In the last equation in (3.19), we have $\overline{\boldsymbol{\sigma}}^s : \overline{\boldsymbol{\sigma}}^s = 2\mu\boldsymbol{D}(\boldsymbol{v}^s) : \boldsymbol{\sigma}^s$ and:

$$\int_{\Omega_s} \frac{1}{4\mu}\overline{\boldsymbol{\sigma}}^s : \overline{\boldsymbol{\sigma}}^s dV = \int_{\Gamma} \frac{1}{2}\boldsymbol{\nu}.\boldsymbol{\sigma}^s.\boldsymbol{v}^s dS \tag{3.30}$$

Owing to Eqs. (3.29) and (3.30) in Eq. (3.19), we obtain:

$$\begin{aligned} W^*(p^d,\boldsymbol{\sigma}^s) = &-\frac{1}{|\Omega|}\int_{\partial\Omega} \frac{1}{2}p^d(\boldsymbol{v}^d.\boldsymbol{n})dS + \frac{1}{|\Omega|}\int_{\Gamma} \frac{1}{2}p^d(\boldsymbol{v}^d.\boldsymbol{\nu})dS \\ &+\frac{1}{|\Omega|}\int_{\Gamma} \frac{1}{2\lambda}(\boldsymbol{\nu}.\boldsymbol{\sigma}^s.\boldsymbol{\tau})^2 dS + \frac{1}{|\Omega|}\int_{\Gamma} \frac{1}{2}\boldsymbol{\nu}.\boldsymbol{\sigma}^s.\boldsymbol{v}^s dS \end{aligned} \tag{3.31}$$

The velocity field $\boldsymbol{v}^s$ is split into its normal and tangential component. Considering additionally the continuity of the normal velocity across Γ, we obtain:

$$\begin{aligned} W^*(p^d,\boldsymbol{\sigma}^s) = &-\frac{1}{|\Omega|}\int_{\partial\Omega} \frac{1}{2}p^d(\boldsymbol{v}^d.\boldsymbol{n})dS + \frac{1}{|\Omega|}\int_{\Gamma} \frac{1}{2}(\boldsymbol{v}^d.\boldsymbol{\nu})\left[\boldsymbol{\nu}.\boldsymbol{\sigma}^s.\boldsymbol{\nu} + p^d\right] dS \\ &+\frac{1}{|\Omega|}\int_{\Gamma} \frac{1}{2}\left[\frac{1}{\lambda}\boldsymbol{\nu}.\boldsymbol{\sigma}^s.\boldsymbol{\tau} + \boldsymbol{v}^s.\boldsymbol{\tau}\right](\boldsymbol{\nu}.\boldsymbol{\sigma}^s.\boldsymbol{\tau})dS \end{aligned} \tag{3.32}$$

The two last integrals are null considering the interface conditions (2.4) and (2.5). It remains:

$$W^*(p^d,\boldsymbol{\sigma}^s) = -\frac{1}{|\Omega|}\int_{\partial\Omega} \frac{1}{2}p^d(\boldsymbol{v}^d.\boldsymbol{n})dS \tag{3.33}$$

On the boundary $\partial\Omega$, we have $p^d = \boldsymbol{J}.\boldsymbol{x}$. Moreover, $\boldsymbol{v}^s$ being divergence free, we have:

$$W^*(p^d,\boldsymbol{\sigma}^s) = -\boldsymbol{J}.\frac{1}{|\Omega|}\int_{\partial\Omega} \frac{1}{2}\boldsymbol{x}(\boldsymbol{v}^d.\boldsymbol{n})dS = -\frac{1}{2}\boldsymbol{J}.\frac{1}{|\Omega|}\int_{\Omega} \boldsymbol{v}^d dS = -\frac{1}{2}\boldsymbol{J}.\boldsymbol{V} \tag{3.34}$$

That is equivalent to (3.28) if we replace $\boldsymbol{V} = -\frac{1}{\mu}\boldsymbol{K}^{hom}.\boldsymbol{J}$

4. The confocal spheroids

In order to determine close form expressions of the macroscopic permeability, a simplified RVE is considered. An axisymmetric spheroidal cavity of semi-axes a_1 and b_1 is embedded in a confocal spheroid of semi-axes a_2 and b_2. The inner spheroid of semi-axes a_1 and b_1 represents the macropore and is fulfilled by the viscous fluid in which the fluid flow obeys to the Stokes equations. The coating (from semi-axes a_1, b_1 to a_2, b_2) is constituted of the microporous medium in which the fluid flow obeys to the Darcy equation. Such a choice allows to recover as a limit, the cases of coaxial cylindrical or spherical voids already studied in Monchiet et al. (24). Fig. 2 depicts the RVE relative to the (x_1, x_2, x_3) cartesian coordinates system (of

orthonormal basis $(\boldsymbol{e}_1, \boldsymbol{e}_2, \boldsymbol{e}_3)$, with axis x_3 aligned with the axis of symmetry of the void. The shape of the cavity is described by the aspect ratio a_1/b_1, with $a_1 > b_1$ corresponding to a prolate cavity while $b_1 > a_1$ corresponds to an oblate one. Let us denote by c the focal distance given by $c = \sqrt{a^2 - b^2}$ for prolate spheroid and by $c = \sqrt{b^2 - a^2}$ for oblate case. The focal distance is the same for the inner and the outer spheroid due to the hypothesis of confocality. We also denote by e the eccentricity of a spheroid defined by $e = c/a$ for prolate spheroid and by $e = c/b$ for oblate one. The eccentricity of the inner spheroid is then denoted e_1, that of the outer spheroid is denoted by e_2. We will use cylindrical coordinates (ρ, θ, z)

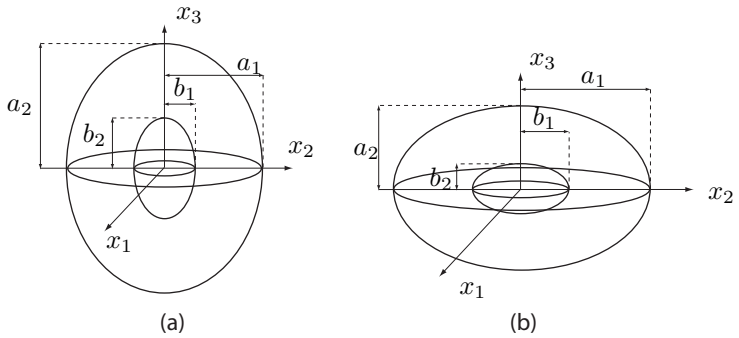

Figure 2. The cell considered (a) a prolate and (b) an oblate spheroidal macropore (with semi-axes a_1, b_1) embedded in a confocal spheroid of semi-axes a_2, b_2 that represents the surrounding microporous medium.

and $(\boldsymbol{e}_\rho, \boldsymbol{e}_\theta, \boldsymbol{e}_z)$ the associated orthonormal basis, also the spheroidal coordinates $(\lambda, \varphi, \theta)$ and the associated orthogonal basis $(\boldsymbol{e}_\lambda, \boldsymbol{e}_\varphi, \boldsymbol{e}_\theta)$. The spheroidal coordinates are related to the cartesian coordinates by:

$$x_1 = b\cos(\theta)\sin(\varphi), \quad x_2 = b\sin(\theta)\sin(\varphi); \quad x_3 = a\cos(\varphi) \tag{4.1}$$

Where $b = c\sinh(\lambda)$ and $a = c\cosh(\lambda)$ in the case of a prolate spheroid while, in the case of an oblate cavity, $a = c\sinh(\lambda)$ and $b = c\cosh(\lambda)$ with $\lambda \in [0, +\infty[$, also $\varphi \in [0, \pi]$ and $\theta \in [0, 2\pi]$. The outer spheroid corresponds to $\lambda = \lambda_2$ while the inner one corresponds to $\lambda = \lambda_1$. The iso-λ surfaces are confocal spheroids.
The unit vectors of the spheroidal basis are:

$$\underline{e}_\lambda = \frac{1}{L_\lambda}\left\{a\sin(\varphi)\ \underline{e}_\rho + b\cos(\varphi)\ \underline{e}_3\right\}; \quad \underline{e}_\varphi = \frac{1}{L_\lambda}\left\{b\cos(\varphi)\ \underline{e}_\rho - a\sin(\varphi)\ \underline{e}_3\right\} \tag{4.2}$$

with $L_\lambda = \sqrt{a^2\sin^2(\varphi) + b^2\cos^2(\varphi)}$.
The porosity f related to the macropores is given by:

$$f = \frac{a_1 b_1^2}{a_2 b_2^2} \tag{4.3}$$

Note that f is not the total porosity since it does not include the porosity related to the micro-channels system. In the case $f = 0$, the volume of the macropore is null and the RVE is only constituted of the population of micropores.

5. Derivation of analytic bounds

We propose to determine a lower and an upper bound of the macroscopic permeability. To this end, we use the kinematic and static approach described in section 3 with appropriate trial fields. The latter are inspired of the exact solution for the spherical shape. Particularly, two constatations could be done regarding the solution in the case of coaxial spheres. First, the solution in the Darcy region has the same general expression that the solution of Eshebly (15; 16) for the problem of thermal conductivity. It is constituted of a first constant field satisfying to a prescribed constant remote velocity and a supplementary heterogeneous field in "$1/r^3$" due to the presence of the spherical inhomogeneity. Due to the equivalence between the Darcy equations and that of the thermal conductivity, we can use the Eshelby solution of the spheroidal inhomogeneity problem as the trial field in the Darcy region. Moreover, this field complies with the two kind of boundary conditions considered in this paper (see section 2b). Second, the solution within the spherical macropore is quadratic with the position vector. Consequently, we also use a quadratic field in the spheroidal macropore.
In this section we present the trial fields considered for the kinematic and static approach. The admissibility conditions are verified and we provide the analytic expressions of the bounds. All the details related to the derivations of the bounds are provided in appendices as supplementary material (see ref. (25)).

(a) *Kinematical approach : lower bound for the macroscopic permeability*

(i) *The field inside the Darcy matrix*

In the Darcy region, the following trial velocity field is considered:

$$v_\lambda = \frac{b}{L_\lambda}\left[D_1 - D_2\Delta(1-\alpha)\right]\cos(\varphi) \tag{5.1}$$

$$v_\varphi = \frac{a}{L_\lambda}\left[D_1 + D_2\Delta\alpha\right]\sin(\varphi) \tag{5.2}$$

$$v_\theta = 0 \tag{5.3}$$

in which $v_\lambda, v_\varphi, v_\theta$ are the components of the velocity field in the spheroidal frame $(\boldsymbol{e}_\lambda, \boldsymbol{e}_\varphi, \boldsymbol{e}_\theta)$. In Eq. (5.1), D_1 and D_2 are two unknown coefficients. Δ is defined by:

$$\Delta = \frac{a_1 b_1^2}{a b^2} \tag{5.4}$$

Particularly, $\Delta = 1$ when $\lambda = \lambda_1$ (at the interface Γ) and $\Delta = f$ when $\lambda = \lambda_2$ (at the boundary of the RVE). In Eq. (5.1), α is also a function of λ (or equivalently the eccentricity e) and is given by:

$$\alpha = \begin{cases} \dfrac{1-e^2}{e^3}\operatorname{arctanh}(e) - \dfrac{1-e^2}{e^2} & \text{(prolate)} \\ -\dfrac{\sqrt{1-e^2}}{e^3}\arcsin(e) + \dfrac{1}{e^2} & \text{(oblate)} \end{cases} \tag{5.5}$$

With the introduction of α we obtain a unique expression for both oblate and prolate cases. This field is inspired of the solution of the spheroidal inhomogeneity

problem embedded in an infinite solid for the thermal conductivity problem. The field associated with coefficients D_1 complies to a remote uniform velocity prescribed at the infinity ($\lambda = +\infty$). The field associated with D_2 is the perturbed heterogeneous field due to the presence of the spheroidal inclusion and vanishes at the infinity.
Consider the particular case of the spherical shape. We use the spherical coordinates (r, φ, θ) and the associated spherical frame $(\boldsymbol{e}_r, \boldsymbol{e}_\varphi, \boldsymbol{e}_\theta)$. We have $a = b = L_\lambda = r$, $c = 0$ and the eccentricity is $e = 0$. By taking the limit in Eq. (5.5), we found that $\alpha = 1/3$. Moreover Δ given by Eq. (5.4) is $\Delta = a_1^3/r^3$ ($a_1 = b_1$ being the radius of the spherical macropore). Component v_λ in Eq. (5.1) becomes the radial component v_r in the spherical frame. The components of the velocity field are then given by:

$$v_r = \left[D_1 - D_2 \frac{2a_1^3}{3r^3}\right] \cos(\varphi) \tag{5.6}$$

$$v_\varphi = \left[D_1 + D_2 \frac{a_1^3}{3r^3}\right] \sin(\varphi) \tag{5.7}$$

$$v_\theta = 0 \tag{5.8}$$

that is the general form of the solution derived in Monchiet et al. (24).

(ii) *Expression in the Stokes region*

In order to recover the solution for the spherical shape, we consider in the Stokes region a velocity field that is quadratic with respect to the position vector. :

$$v_1 = S_2 x_1 x_3 \tag{5.9}$$

$$v_2 = S_2 x_2 x_3 \tag{5.10}$$

$$v_3 = S_1 + S_3(x_1^2 + x_2^2) - S_2 x_3^2 \tag{5.11}$$

where v_1, v_2, and v_3 are the component of the velocity field written in the cartesian frame.
The velocity considered in the Darcy and in the Stokes region contains the exact solution for the spherical shape. As a consequence, the macroscopic permeability derived from the minimum principle becomes exact in the case of a spherical macropore.
The components of the velocity field, written in the spheroidal frame, are:

$$v_\lambda = \frac{b}{L_\lambda}\left[S_1 + S_2 a^2(1 - 2\cos(\varphi)^2) + S_3 b^2 \sin(\varphi)^2\right] \cos(\varphi) \tag{5.12}$$

$$v_\varphi = \frac{a}{L_\lambda}\left[S_1 - S_2(a^2 + b^2)\cos(\varphi)^2 + S_3 b^2 \sin(\varphi)^2\right] \sin(\varphi) \tag{5.13}$$

$$v_\theta = 0 \tag{5.14}$$

(iii) *Verification of boundary conditions*

Let us recall that the trial velocity field must comply with the uniform velocity boundary conditions (2.13). At the boundary, we have $\lambda = \lambda_2$, $\Delta = f$ and $\alpha = \alpha_2$. Te verification of the boundary condition leads to:

$$D_1 - D_2 f(1 - \alpha_2) = V_3 \tag{5.15}$$

(iv) *Continuity of the normal velocity at the interface*

Additionally, the normal component of the velocity field must be continuous across the interface Γ. This involves the continuity of the component v_λ at $\lambda = \lambda_1$. It leads to:

$$D_1 - D_2(1-\alpha_1) = S_1 + S_2 a_1^2 + S_3 b_1^2, \tag{5.16}$$

$$2S_2 a_1^2 + S_3 b_1^2 = 0 \tag{5.17}$$

Let us introduce the following change of variables:

$$S_2 = \frac{S_2'}{a_1^2} \quad S_3 = -\frac{2S_2'}{b_1^2} \tag{5.18}$$

Eqs. (5.16) and (5.17) become:

$$D_1 - D_2(1-\alpha_1) = S_1 - S_2' \tag{5.19}$$

(v) *Derivation of the macroscopic permeability*

At this stage, the velocity defined by Eqs. (5.1) and (5.9) contains five coefficients D_1, D_2, S_1, S_2 and S_3. In fact, the trial field depends on two independent coefficients after verification of the boundary condition (see Eq. (5.15)) and the interface condition (see Eqs. (5.18) and (5.19)). The remaining unknown coefficients are determined by the minimization of $W(\boldsymbol{v})$ defined by Eq. (3.1). In (25), we provide all the details about the calculation of the volume and surface integrals which enters in $W(\boldsymbol{v})$. Also, the minimization of $W(\boldsymbol{v})$ with respect to the unknown coefficients is subsequently provided and the macroscopic permeability is derived. Below, are given the analytic results.
The macroscopic longitudinal permeability is:

$$K_{33}^{hom} = k\left[1 + \frac{f}{\alpha_1 - f\alpha_2 - T}\right] \tag{5.20}$$

In Eq. (5.20), it is recalled that k is the permeability of the surrounding solid, α_1 and α_2 are the values of α given by Eq. (5.5) for $e = e_1$ and $e = e_2$ respectively. Expression of T is:

$$T = \frac{\gamma_1\beta\delta\epsilon^2 + (\gamma_1\gamma_3 - \gamma_2^2)\delta^2\epsilon}{\gamma_1\beta\delta\epsilon^2 + (\gamma_1\gamma_3 - \gamma_2^2)\delta^2\epsilon - \beta\epsilon - (\gamma_1 - 2\gamma_2 + \gamma_3)\delta} \tag{5.21}$$

In which β, γ_1, γ_2, γ_3 are four coefficients which depend on the eccentricity e_1 of the inner spheroid. Their expressions are:

$$\begin{aligned}
\gamma_1 &= \frac{3}{2}\frac{(1-t)a_1^2 + 2tb_1^2}{a_1 b_1}, \\
\gamma_2 &= \frac{3}{8}\frac{7(1-t)a_1^2 + 2(1+6t)b_1^2}{a_1 b_1} \\
\gamma_3 &= \frac{1}{16}\frac{75(1-t)a_1^4 + 6(6+19t)a_1^2 b_1^2 + 4b_1^4}{a_1^3 b_1}
\end{aligned} \tag{5.22}$$

with:

$$t = \begin{cases} -\dfrac{\sqrt{1-e^2}}{e^3}\arcsin(e) + \dfrac{1}{e^2} & \text{(prolate)} \\ \dfrac{1-e^2}{e^3}\operatorname{arctanh}(e) - \dfrac{1-e^2}{e^2} & \text{(oblate)} \end{cases} \tag{5.23}$$

In Eq. (5.21), it is recalled that δ is the slip coefficient introduced in Eq. (2.7). Moreover $\epsilon = \sqrt{k}/b_1$ in which $k = 1/h$ is the permeability of the permeable surrounding solid. Note that $k \sim d^2$ where d is the characteristic length of the second porosity. Consequently $\epsilon \sim d/b_1$. Due to the separation of scale between the two porosities, ϵ is a small parameter called "scale factor between the two porosities".

(b) *Static approach: upper bound for the macroscopic permeability*

(i) *The field in the Darcy region*

In the Darcy region, we choose the pressure field into the form:

$$p^d = a\,[D_1^* + D_2^*\Delta\alpha]\cos(\varphi) \tag{5.24}$$

Again this field is adapted from the problem of the spheroidal inhomogeneity problem in an infinite solid in the case of the thermal conductivity. The term related to coefficient D_1^* is associated with a remote constant gradient of pressure while the term related to coefficient D_2^* is the perturbed field due to the presence of the spheroidal inhomogeneity.
The boundary condition (2.9) at $\lambda = \lambda_2$ is satisfied if:

$$D_1^* + D_2^* f\alpha_2 = J_3 \tag{5.25}$$

(ii) *The field in the Stokes region*

In the Stokes region, we choose the stress field in the form:

$$\boldsymbol{\sigma}^s = \begin{pmatrix} S_1^* x_3 & 0 & S_2^* x_1 \\ 0 & S_1^* x_3 & S_2^* x_2 \\ S_2^* x_1 & S_2^* x_2 & -2S_2^* x_3 \end{pmatrix} \tag{5.26}$$

in the cartesian frame $(\boldsymbol{e}_1, \boldsymbol{e}_2, \boldsymbol{e}_3)$. Again, this general expression contains the exact solution for the coaxial spheres. As a consequence, the expression of the macroscopic permeability derived from the static approach becomes exact in the case of the spherical shape.

(iii) *Continuity of the traction at the interface*

Note that the admissibility requires the continuity of the traction at $\lambda = \lambda_1$. It is satisfied for:

$$D_1^* + D_2^*\alpha_1 = \frac{[a_1^2 S_1^* + 2b_1^2 S_2^*]\sin^2(\varphi) - 2b_1^2 S_2^*\cos^2(\varphi)}{L_{\lambda 1}^2} \tag{5.27}$$

It involves:

$$D_1^* + D_2^* \alpha_1 = q S_1^*, \quad S_2^* = -\frac{q}{2} S_1^* \tag{5.28}$$

in which the coefficient q is given by:

$$q = \frac{a_1^2}{a_1^2 + b_1^2} \tag{5.29}$$

(iv) *Macroscopic permeability*

The trial field is defined by the pressure field given by Eq. (5.24) in the Darcy region and by the stress field given by Eq. (5.26) in the Stokes region. These fields then contains four coefficients D_1^*, D_2^*, S_1^* and S_2^*. The admissibility of this trial field includes the verification of the boundary condition for the pressure field (see Eq. (5.25)) and the continuity of the traction at the interface between the regions (see Eq. (5.28)). As a consequence, only one unknown coefficient remains in the problem. This coefficient is determined by the minimization od $W^*(p^d, \boldsymbol{\sigma}^s)$ defined by Eq. (3.18). All the details related to the calculation of the integrals in the expression of $W^*(p^d, \boldsymbol{\sigma}^s)$ and its minimization with the undetermined coefficient are provided in the appendices which can be found in (25). Also, the derivation of the macroscopic permeability is detailed. The final results are summarized below.
The macroscopic permeability reads:

$$K_{33}^{hom} = k \left[1 + \frac{f}{\alpha_1 - f\alpha_2 - T^*} \right] \tag{5.30}$$

with :

$$T^* = \frac{q^2 \delta \epsilon^2}{q^2 \delta \epsilon^2 - \gamma^* \epsilon - \beta^* \delta} \tag{5.31}$$

Expression of T^* depends on q, γ^* and β^* which depend on the eccentricity of the inner spheroid. Coefficient q is given by Eq. (5.29). Coefficients γ^* and β^* are given by:

$$\gamma^* = \frac{3a_1^3(3(1-t)a_1^2 + 2(1+2t)b_1^2)}{32 b_1 (a_1^2 + b_1^2)^2}; \quad \beta^* = \frac{a_1^2(3a_1^2 + 2b_1^2)}{30(a_1^2 + b_1^2)^2} \tag{5.32}$$

and t is given by Eq. (5.23). Note that T^* also depends on the slip coefficient δ and on the scale factor $\epsilon = \sqrt{k}/b_1$.

6. Illustrations

In Fig. 3 and Fig. 4 we represent the variations of the macroscopic longitudinal resistivity as function of the volume fraction f of the macropores. On each figures, we consider different values of the aspect ratio : $a_1/b_1 = 1/5, 1/2, 1, 2, 5$. Also, we used different values of the scale factor $\epsilon = \sqrt{k}/b_1$ and of the slip coefficient δ. The particular case $a_1 = b_1$ correspond to the spherical shape for which the two bounds coincide with the exact solution derived in (24). On each figure, we represent

the resistivity obtained with the kinematic approach (the upper bound) and with the static approach (the lower bound). Let us recall that the kinematic approach delivers an upper bound for the macroscopic permeability, then a lower bound for the resistivity and vice versa for the static approach.

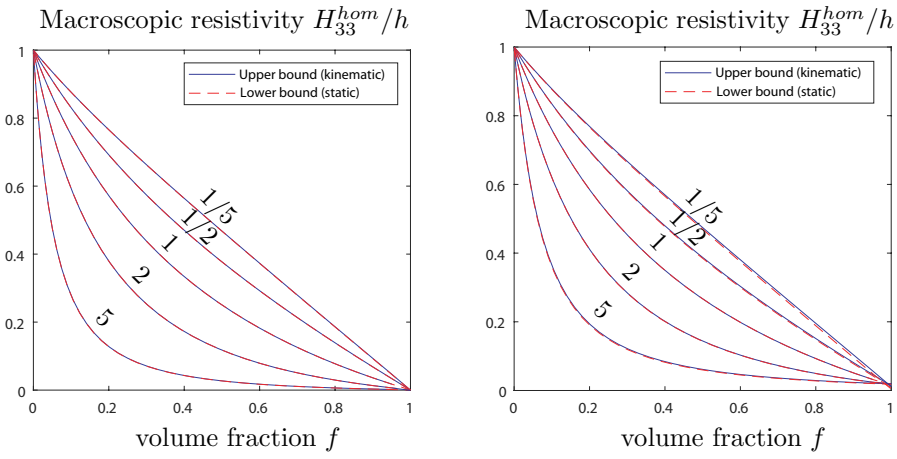

Figure 3. Variations of the macroscopic hydraulic resistivity as function of the macropore volume fraction (see Eq. (4.3)) for different spheroidal shapes, $\delta = 0.1$ and $\epsilon = 0.01$ (at the left) and $\epsilon = 0.1$ (at the right).

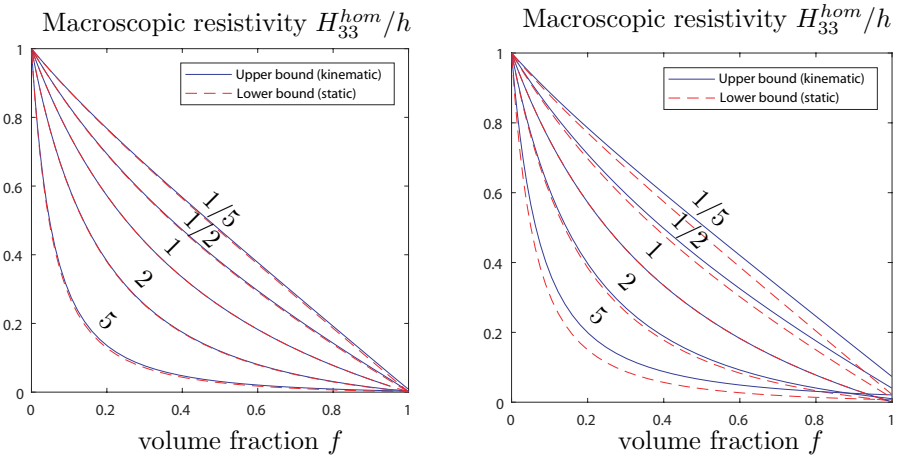

Figure 4. Variations of the macroscopic hydraulic resistivity as function of the macropore volume fraction (see Eq. (4.3)) for different spheroidal shapes, $\epsilon = 0.01$, $\delta = 1$ (at the left) and $\delta = 10$ (at the right).

It is observed that, at a given value of the porosity f and comparatively to the spherical shape, an oblate spheroidal shape increases the resistivity (then reduces the permeability) while a prolate spheroidal shape decreases the resistivity (then increases the macroscopic permeability). Obviously, this remark only holds

for the longitudinal resistivity, i.e. along the axe of revolution of the spheroid. The transverse permeability has not been determined in this paper and such observation would probably be inverted in that case. The transverse permeability will be derived in a future work. It observed in Figs. 3 and 4 that the lower and upper bounds are very closed in the great majority of cases. For the considered values of δ and ε, the bounds then provide a good estimation of the exact solution. However, in the last Fig. 4 (at the right) some important differences are noted particularly when the aspect ratio is equal to 1/5 (oblate void) and 5 (prolate void). In that case the variations of the macroscopic longitudinal resistivity are represented for a higher value of the slip coefficient ($\delta = 10$) than in other figures. The solution could be perhaps improved by considering additional trial fields in the Stokes region, not in the Darcy region, since the BJS interface condition only involves the velocity $\boldsymbol{v}^s$. Further investigations could be carried on to improve the bounds in the case of large values of the slip coefficient.

7. Conclusion

In this paper, we derive analytic expression of the macroscopic longitudinal permeability of doubly porous materials made up of an initially isotropic permeable solid in which spheroidal macropores are embedded. The homogenization problem consists to solve, at the intermediate scale, the coupled Darcy/Stokes equations with the Beavers-Joseph-Saffman (BJS) interface model. Two variational procedures are provided to determine a lower and an upper bound for the macroscopic permeability of the doubly material. The approach is applied in the case of confocal spheroids that corresponding to a simplified representation of the real microstructure. By choosing the appropriate trial fields, two close form expressions of the macroscopic longitudinal permeability are derived which, particularly, leads to the exact solution in the particular case of coaxial spheres.
The results shown that the two bounds are very closed in the large range of the physical parameters which enter in the expression of the permeability : the volume fraction of the macropores, the eccentricity of the spheroidal macropores, the scale factor between the two population of pores and the slip coefficient of the BJS model. It must be however noted significant differences for large values of the slip coefficient.
In order to evaluate the accuracy of the approximate expressions, the comparison with numerical solutions could be provided. Moreover the results must be also extended to the case of non axisymmetric loading in order to determine the transverse permeability. This will be the subjects of the next work.

There is no acknowledgements and no funding was received for this research.

References

[1] Arbogast T, Lehr HL. 2006 Homogenization of a Darcy-Stokes systen modeling vuggy porous media. *Comput. Geosciences.* 10(3):291-302.

[2] Arbogast T, Brunson DS. 2007 A computatonal method for approximating a Darcy-Stokes system governing a vuggy porous medium. *Comput. Geosciences.* 11(3):207-218.

[3] Auriault JL, Sanchez-Palencia E. 1977 Study of macroscopic behavior of a deformable porous medium. *J. Méca.* 16(4):575-603.

[4] Auriault JL, Boutin C. 1992 Deformable porous media with double porosity. Quasi-statics. I: Coupling effects. *Transp. Porous Med.* 7:63-82.

[5] Auriault JL, Boutin C. 1993 Deformable porous media with double porosity. Quasi-statics. II: Memory effects. *Transp. Porous Med.* 10:153-169.

[6] Auriault JL, Boutin C. 1994 Deformable porous media with double porosity III: Acoustics. *Transp. Porous Med.* 14:143-162.

[7] Auriault JL, Geindreau C, Boutin C. 2005 Filtration law in porous media with poor separation of scales. *Transp. Porous Med.* 60(1):89-108.

[8] Barrenblatt GI, Zheltov IP, Kochina IN. 1960 Basic concepts in the theory of seepage of homogeneous liquids in fissured rocks. *Prikladnaya Matematica y Mechanica.* 24:852-864.

[9] Beavers GS, Joseph DD. 1967 Boundary condition at a naturally permeable wall. *J. Fluid Mech.* 30(1):197-207.

[10] Bernardi C, Hecht F, Pironneau O. 2005 Coupling Darcy and Stokes equations for porous media with cracks. *ESAIM: Mathematical Modelling and Numerical Analysis.* 39(1):7-35.

[11] Boutin C, Royer P, Auriault JL. 1998 Acoustic absorption of porous surfacing with dual porosity. *Int. J. Solids Structures.* **34**:4709-4737.

[12] Brinkman HC. 1949 A calculation of the viscous force exerted by a flowing fluid on a dense swarm of particles. *App. Sci. Res.* A(1):27-34.

[13] Brinkman HC. 1949 On the permeability of media consisting of closely packed porous particles. *App. Sci. Res.* A(1):81-86.

[14] Eshelby JD. 1957 The determination of the elastic field of an ellipsoidal inclusion and related problem. *Proc. R. Soc. London.* A 241 376-396.

[15] Eshelby JD. 1959 The elastic field outside an ellipsoidal inclusion. *Proc. Roy. Soc. London.* A 252 561-569.

[16] Hanspal NS, Waghode AN, Nassehi V, Wakemann RJ. 2006 Numerical Analysis of Coupled Stokes/Darcy. Flows in Industrial Filtrations *Transp. Porous Med.* 64:73-101.

[17] Ly HB, Le Droumaguet B, Monchiet V, Grande D. 2015 Designing and modeling doubly porous polymeric materials. European Physical Journal. *Eur. Phys. J.* 224(9):1689-1706.

[18] Ly HB, Le Droumaguet B, Monchiet V, Grande D. 2015 Facile fabrication of doubly porous polymeric materials with controlled nano- and macro-porosity. *Polymer.* 78(5):13-21.

[19] Markov M, Kazatchenko E, Mousatov A, Pervago E. 2010 Permeability of the Fluid-Filled Inclusions in Porous Media. *Transp. Porous Med.* 84:307-317.

[20] Maxwell JC. 1873. A Treatise on Electricity and Magnetism. Oxford United Kingdom: Clarendon Press. 31:365-367.

[21] Moctezuma-Berthier A, Vizika O, Adler PM. 2002 Macroscopic conductivity of vugular porous media. *Transp. Porous Med.* 49:313-332.

[22] Moctezuma-Berthier A, Vizika O, Thovert JF, Adler PM. 2004 One- and Two-Phase Permeabilities of Vugular Porous Media. *Transp. Porous Med.* 56:225-244.

[23] Monchiet V, Ly HB, Grande D. 2019 Macroscopic permeability of doubly porous materials with cylindrical and spherical macropores. *Meccanica.* 54(10):1583-1596.

[24] Monchiet V 2020 Data from: Details about the derivation of the lower and upper bound of the permeability of biporous solids with spheroidal macropores. Dryad Digital Repository.

[25] Olny X, Boutin C. 2003 Acoustic wave propagation in double porosity media. *J. Acoust. Soc. Am.* 114(1):73-89.

[26] Popov P, Qin G, Bi L, Efendiev Y, Ewing R, Li J, Efendiev Y, Kang Z, Li J. 2009 Multiphysics and Multiscale Methods for Modeling Fluid Flow Through Naturally Fractured Carbonate Karst Reservoirs. *SPE Reservoir Evaluation & Engineering.* 12(2):218-231.

[27] Raja Sekhar G, Sano O. 2000 Viscous flow past a circular/spherical void in porous mediaŮan application to measurement of the velocity of groundwater by the single boring method. *J. Phys. Soc. Jpn.* 69(8):2479-2484.

[28] Raja Sekhar G, Sano O. 2003 Two-dimensional viscous flow in a granular material with a void of arbitrary shape. *Phys. Fluids* 15:554-567.

[29] Rasoulzadeh M, Kuchuk FJ. 2017 Effective Permeability of a Porous Medium with Spherical and Spheroidal Vug and Fracture Inclusions *Transp Porous Med.* 116:613-644.

[30] Royer P, Auriault JL, Boutin C. 1996 Macroscopic modeling of double-porosity reservoirs. *J. Petroleum Sc. Engrg.* 16:187-202.

[31] Saffman PG. 1971 On the boundary condition at the interface of a porous medium. *Stud. Appl. Math.* **1**: 93-101.

[32] Sahraoui M, Kaviany M. 1992 Slip and no slip velocity boundary conditions at interface of porous plain media. *Int. J. Heat Mass Transfer.* **35(4)**:927-943.

[33] Silva G, Ginzburg I. 2016 Stokes-Brinkman-Darcy solutions of bimodal porous flow across periodic array of permeable cylindrical inclusions: cell model lubrication theory and LBM/FEM numerical simulations. *Transp. Porous Media.* 111(3):795-825.

[34] Wieck J, Person M, Strayer L. 1995 A finite elementmethod for simulating fault blockmotion and hydrothermal fluid flow within rifting basins. *Water Resour. Res.* 31(12):3241-3258.

[35] Zhao C, Valliappan S. 1994 Numerical modelling of transient contaminant migration problems in infinite porous fractured media using finite/infinite element technique. Part II: parametric study. *Int. J. Numer. Anal. Methods Geomech.* 18(8):543-564.